RESEARCH PAPER

Fly7:4, 267–279; October/November/December 2013; © 2013 Landes Bioscience

Mutations in palmitoyl-protein thioesterase 1 alter exocytosis and endocytosis at synapses in *Drosophila* larvae

Elizabeth Aby[1], Katherine Gumps[2], Amalia Roth[1], , Stacey Sigmon[2], Sarah E Jenkins[1], Joyce J Kim [1], Nicholas J Kramer[3], Karen D Parfitt[1,4], and Christopher A Korey[2,*]

[1]Department of Biology; Pomona College; Claremont, CA USA; [2]Department of Biology; The College of Charleston; Charleston, SC USA; [3] Department of Neuroscience; Pomona College; Claremont, CA USA; [4] Program in Molecular Biology ; Pomona College; Claremont, CA USA;

Keywords: *Drosophila*, infantile neuronal ceroid lipofuscinosis, Batten disease, palmitoyl-protein thioesterase-1, synaptic vesicle cycling, endocytosis, exocytosis

Abbreviations: INCL, infantile-onset neuronal ceroid lipofuscinosis; NCL, neuronal ceroid lipofuscinoses; Ppt1, palmitoyl protein-thioesterase 1; CSP, cysteine string protein; NMJ, neuromuscular junction; EJPs, excitatory junctional potentials; shi, shibire

Infantile-onset neuronal ceroid lipofuscinosis (INCL) is a severe pediatric neurodegenerative disorder produced by mutations in the gene encoding palmitoyl-protein thioesterase 1 (Ppt1). This enzyme is responsible for the removal of a palmitate group from its substrate proteins, which may include presynaptic proteins like SNAP-25, cysteine string protein (CSP), dynamin, and synaptotagmin. The fruit fly, *Drosophila melanogaster,* has been a powerful model system for studying the functions of these proteins and the molecular basis of neurological disorders like the NCLs. Genetic modifier screens and tracer uptake studies in *Ppt1* mutant larval garland cells have suggested that Ppt1 plays a role in endocytic trafficking. We have extended this analysis to examine the involvement of Ppt1 in synaptic function at the *Drosophila* larval neuromuscular junction (NMJ). Mutations in *Ppt1* genetically interact with temperature sensitive mutations in the *Drosophila* dynamin gene *shibire,* accelerating the paralytic behavior of *shibire* mutants at 27 °C. Electrophysiological work in NMJs of *Ppt1*-deficient larvae has revealed an increase in miniature excitatory junctional potentials (EJPs) and a significant depression of evoked EJPs in response to repetitive (10 hz) stimulation. Endocytosis was further examined in *Ppt1*-mutant larvae using FM1–43 uptake assays, demonstrating a significant decrease in FM1–43 uptake at the mutant NMJs. Finally, *Ppt1*-deficient and *Ppt1* point mutant larvae display defects in locomotion that are consistent with alterations in synaptic function. Taken together, our genetic, cellular, and electrophysiological analyses suggest a direct role for Ppt1 in synaptic vesicle exo- and endocytosis at motor nerve terminals of the *Drosophila* NMJ.

Introduction

S-Palmitoylation is one of several posttranslational lipidation reactions that occur on specific cellular substrates including both cytoplasmic and integral membrane proteins (for a review, see ref. 1). The addition of the palmitate moiety occurs on particular cysteines via a thioester bond and, unlike myristolation or prenylation, palmitoylation is a modification that can dynamically modulate the function and localization of proteins within the cell. The palmitoylation cycle is controlled by 2 sets of enzymes, the DHHC family of palmitoyl acyl-transferases that add palmitate to particular substrates, and palmitoyl acyl-thioesterases, which remove palmitate. Both enzymes have been implicated in the development of neurological disorders.[2,3] Mutations that alter the function of the Palmitoyl protein-thioesterase 1 (Ppt1) protein are the cause of a childhood neurodegenerative disorder called infantile-onset neuronal ceroid lipofuscinosis.[4]

The neuronal ceroid lipofuscinoses (NCL), more commonly known as the Batten Diseases, are a group of recessive lysosomal storage disorders that produce lipofuscin-like inclusions in all cells and neurodegeneration in the cerebellum, retina, and cerebral cortex.[5] To date, 14 different forms have been characterized primarily by their age of onset and cellular inclusion pathology.[6] The infantile onset form of the disease (INCL) is one of the more severe forms, with symptoms such as blindness, ataxia, and mental decline beginning to appear by 6–12 mo of age.[7-9] Mutations in the soluble lysosomal enzyme Ppt1 are the underlying molecular cause of the disease, but it is still unclear why the loss of this ubiquitously expressed protein produces a very specific neurodegenerative phenotype.[4] The disease phenotype provides further support that efficient

*Correspondence to: Christopher A Korey; Email: koreyc@cofc.edu
Submitted: 07/10/2013; Revised: 09/14/2013; Accepted: 09/26/2013
http://dx.doi.org/10.4161/fly.26630

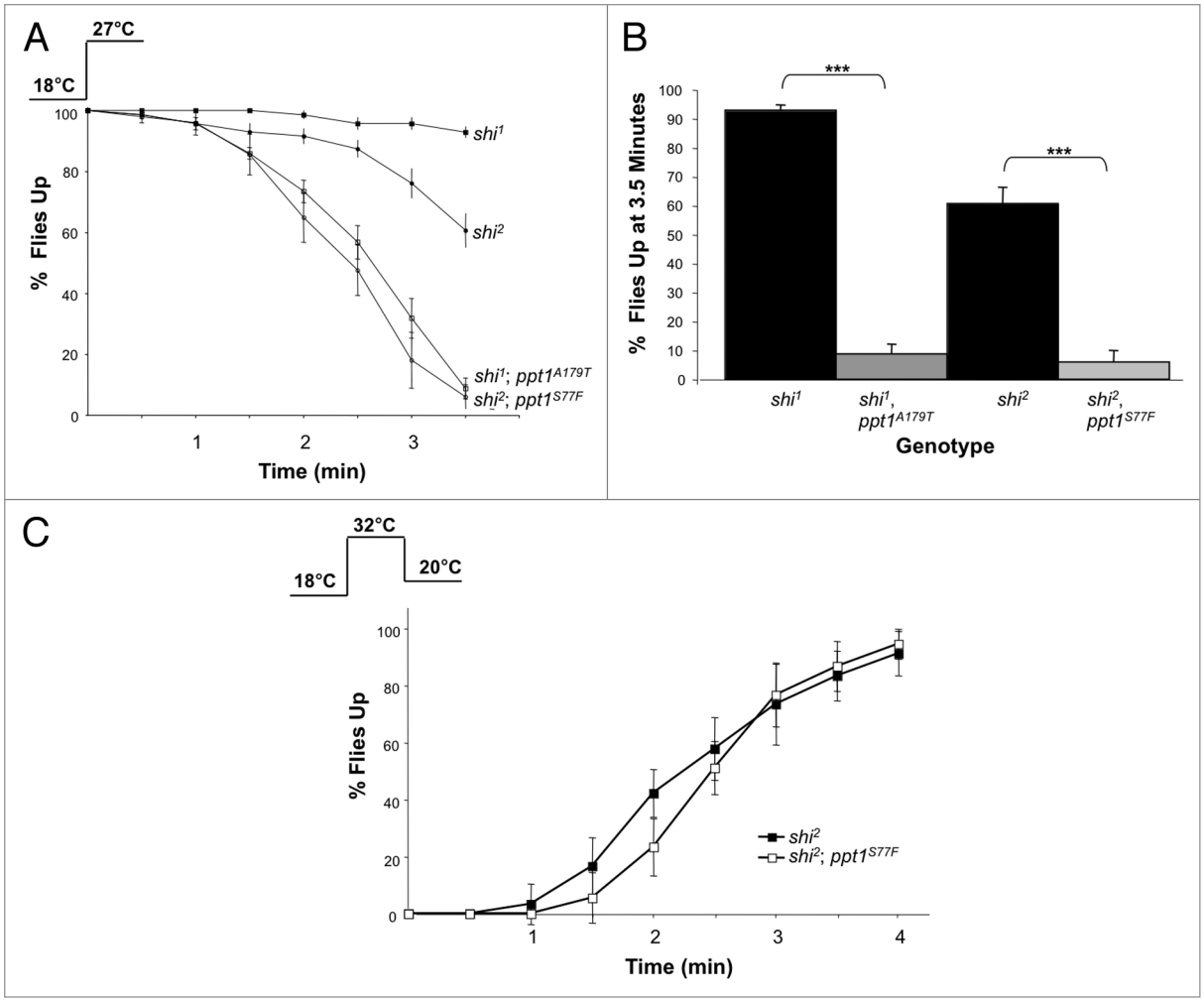

Figure 1. *Ppt1* and *shibire* genetically interact. (**A**) *shibire* and *Ppt1* double mutant chromosomes were characterized in a standard paralysis assay. The graph shows the paralysis profiles for *shibire* mutants alone and *shibire-ppt1* double mutants. n = 7 for $shi_{,}^{1}$ n = 7 for $shi_{,}^{2}$ n = 7 for shi^{1}; $Ppt1^{A179T}$, and n = 5 for shi^{2}; $Ppt1^{S77F}$ where n = number of vials with 10 male flies/vial. (**B**) For each genotype, we calculated the percentage of flies remaining up after 3.5 min. Double mutants paralyzed significantly faster than *shibire* mutants alone (*** $p < 0.001$). (**C**) The graph shows the percentage of flies standing over the time course of a paralysis recovery at 20 °C. Both genotypes (shi^{2} *and* shi^{2}; $ppt1^{S77F}$) were placed in vials with 10 flies each. The flies were kept at 18 °C, heat shocked at 32 °C for 2 min, then moved to 20 °C for recovery. After each 30 s interval the number of flies up was recorded and percentages were calculated. n = 9 for for shi^{2} and shi^{2}; $Ppt1^{S77F}$ where n = number of vials. Double mutant flies showed no significant difference in recovery times as compared with *shibire* alone.

modulation of protein palmitoylation is crucial for normal neuronal function.[10]

The use of several different model systems, in particular yeast, *Drosophila*, and mice, has begun to shed light on the cellular function of Ppt1 and the role of palmitoylation in neuronal development and synaptic transmission (reviewed in ref. 11). *Drosophila melanogaster* has proven to be an invaluable tool for dissecting the molecular etiology of human neurological disorders (reviewed in refs. 12–14). This has also been the case for lysosomal storage disorders where both gain-of-function and loss-of-function genetic models have been produced for Congenital NCL (*Ctsd*),[15,16] INCL[17,18] and Juvenile NCL (*Cln3*).[19,20] Mutations in *Drosophila* that mimic the Ppt1 loss-of-function seen in human INCL produce cytoplasmic inclusions and autoflourescent storage material.[17] Embryological characterization of these mutations in the fly demonstrates a role for *Ppt1* in early neuronal specification and axon guidance.[21] Gain-of-function genetic screens in the fly have implicated *Ppt1* function in the regulation of several neuronal processes, including synaptic growth/homeostasis and synaptic vesicle endo/exocytosis.[22,23] An examination of non-neuronal larval garland cells in *Ppt1* mutants showed reduced endocytosis rates, without alterations in endo-lysosomal trafficking.[23] Similarly, alterations in endocytosis have been observed in fibroblasts from INCL patients.[24] In neural tissue, changes in endocytosis have been reported in cultured neurons of *Ppt1*-deficient mice and humans in the context of a reduction in the synaptic vesicle pool size, but the functional consequences of *Ppt1* mutations on endocytosis remains to be characterized.[25,26]

Many proteins involved in synaptic vesicle endo- and exocytosis such as dynamin, endophylin A, SNAP-25, synaptotagmin, the

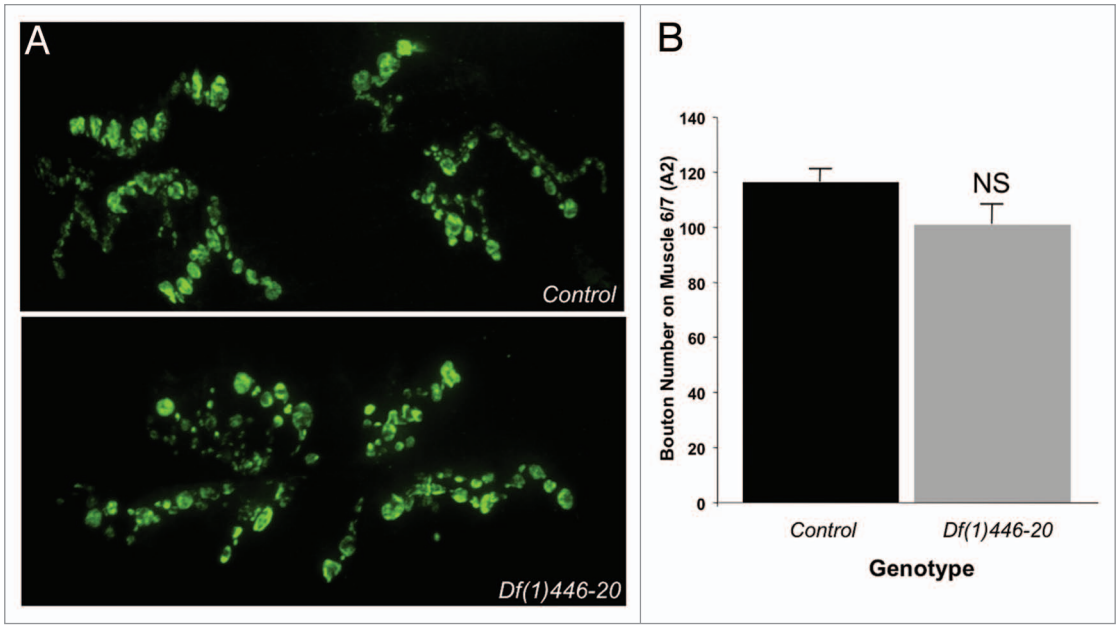

Figure 2. Ppt1 mutations do not alter synaptic structure. (**A**) Images of *wild type* and *Df(1)446–20* neuromuscular junctions from wandering 3rd instar larval muscles 6 and 7 in abdominal segment A2. Synaptic boutons were visualized with an anti-synaptotagmin antibody. No obvious morphological defects are seen at *Df(1)446–20* synapses. (**B**) A graph of bouton counts (average+/–SE) from the same muscle set shown in (**A**). There is no significant statistical difference in the number of boutons between the 2 genotypes (p = 0.11, Mann-Whitney). n = 9 larvae for both wild type and *Df(1)446–20*.

cysteine string protein (CSP), and synaptobrevin 2 (VAMP2) are likely substrates of Ppt1, and the membrane localization of these proteins may be influenced by their palmitoylation status. Kim et al.[26] have observed reduced levels of many of these presynaptic proteins in the soluble fraction of postmortem brains of INCL patients, as well as in Ppt1-knockout mice, suggesting that these proteins remain anchored to the synaptic membrane in the absence of depalmitoylation. Palmitoylation also seems to play a role in the correct localization of presynaptic proteins to the appropriate intracellular or plasma membrane domain, as shown in the *Drosophila* mutant of palmitoyl acyl transferase, *hip14*.[27] In these mutants, the inability to palmitoylate CSP and SNAP-25 leads to the mislocalization of these proteins such that they remain in the neuronal cell bodies instead of being trafficked to the nerve terminals.[27,28] As a result, these palmitoylation mutants also show defects in synaptic vesicle exocytosis.

In this study, we have examined the consequences of *Ppt1* mutations at the *Drosophila* larval neuromuscular junction, a very well-characterized synapse. We initially observed genetic interactions between *Ppt1* mutations and *Dynamin* temperature sensitive alleles and subsequently found changes in spontaneous release of glutamate from the motor nerve terminals, as well as altered responses to repetitive stimulation of the motor nerve. Changes in endocytosis/vesicle recycling were demonstrated in vivo by a reduced ability of nerve terminals to recover from repetitive stimulation and by reductions in FM1–43 uptake in the *Ppt1*-mutant larval nerve terminals. Finally, we have observed defects in larval locomotion in *Ppt1*-deficient larvae, which were rescued by neuronal expression of Ppt1. These data point to the importance of *Ppt1*, and palmitoylation in general, in synaptic vesicle endo- and exocytosis and neuromuscular function.

Results

Ppt1 significantly enhances the *shibire* paralytic phenotype

In order to further probe Ppt1 connection to vesicle endocytosis genes that had been revealed in genetic modifier screens, we turned to temperature sensitive loss-of-function mutations in the *shibire (shi)* locus, which encodes the *Drosophila* Dynamin homolog.[29] Our previous work demonstrated a gain-of-function genetic interaction with the Dynamin gene. The $shibire^{ts1}$ (shi^{1}) and $shibire^{ts2}$ (shi^{2}) alleles show reversible paralysis when shifted to 29 °C caused by adverse effects on endocytosis and a temporary block in synaptic vesicle recycling.[30,31] Alleles of *Ppt1* show no paralysis at elevated temperatures (data not shown). To examine loss-of-function genetic interactions between alleles of *Ppt1* and *shi* we created double mutant $shi,^{1}$ $Ppt1^{A179T}$ and $shi,^{2}$ $Ppt1^{S77F}$ X-chromosomes using meiotic recombination (see Materials and Methods for selection procedures). Previous work has shown that 27 °C provides a sensitized background in which to observe modifications of the *shi* paralysis profile.[32] We performed assays to measure paralysis and recovery rates of 4 *Drosophila* lines (shi^{1}; shi^{2}; $shi,^{1}$ $Ppt1^{A179T}$ and $shi,^{2}$ $Ppt1^{S77F}$). When individual lines were held at 18 °C and then shifted to 27 °C, an increase in the rate of paralysis was observed when comparing the single *shi* mutants (7 vials) to the *shi, Ppt1* double mutants (7 vials) (**Fig. 1A–B**). The percentage of non-paralyzed $shi,^{1}$ $Ppt1^{A179T}$ was significantly reduced (8.7% +/− 3.4) as compared with non-paralyzed shi^{1} flies (92.9% +/− 1.8) at the 3.5 min time point ($p < 0.001$, Student t-test). Consistent with this interaction, the percentage of non-paralyzed $shi,^{2}$ $Ppt1^{S77F}$ flies (6.0% +/− 4; 5 vials) was significantly reduced as compared with non-paralyzed shi^{2} flies (60.6% +/− 5.6; 7 vials) at 3.5 min

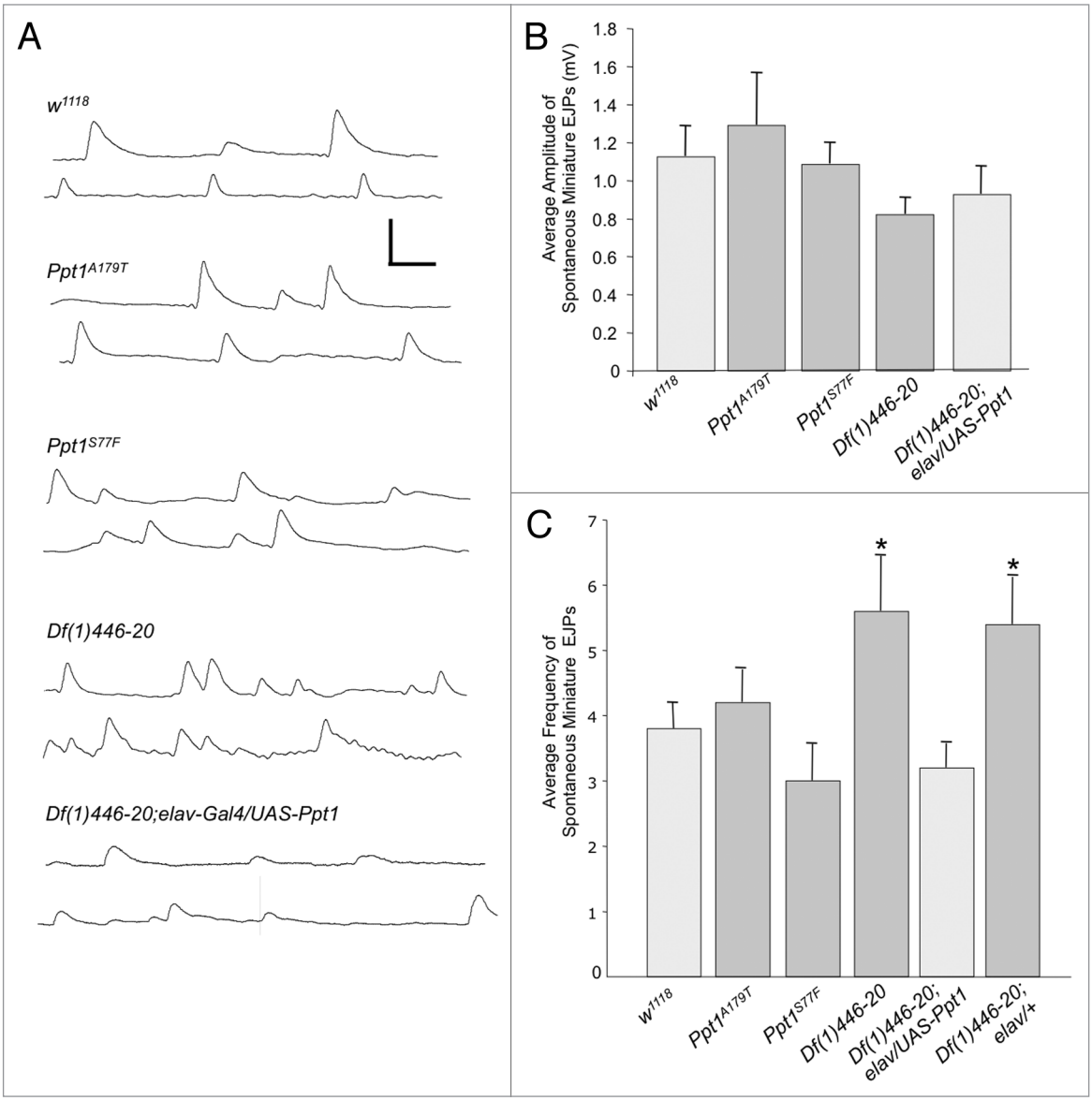

Figure 3. Synapses of Ppt1-deficient mutants display increases in spontaneous neurotransmitter release. (**A**) Representative traces of spontaneous miniature EJPs in muscle 6 of w^{1118}, $Ppt1^{A179T}$, $Ppt1^{S77F}$, *Df(1)446–20* and *Df(1)446–20;elav-Gal4/UAS-Ppt1* larvae. Scale bars are 1 mV, 100 ms. (**B**) Average amplitudes of mini EJPs from the genotypes indicated. Averages were obtained from 10–20 cells per genotype. No significant differences between genotypes were observed. (**C**) Average miniature EJP frequency for the genotypes listed, obtained from 10–20 cells per genotype. The average mini EJP frequency was significantly higher in cells from *Df(1)446–20 and Df(1)446–20;elav/+* larvae (* = $p < 0.05$, 1-way ANOVA) and were not significantly different from w^{1118} in $Ppt1^{A179T}$, $Ppt1^{S77F}$, or *Df(1)446–20;elav-Gal4/UAS-Ppt1* larvae .

($p > 0.001$, Student t-test). These results are representative of 3 independent, blind experiments. We also determined whether *Ppt1* mutations alter the paralytic recovery rate of *shibire* mutations. Synaptic vesicles that have been depleted at restrictive temperatures in *shi* mutants recover, and recycling events are restored, once the flies are shifted to the permissive temperatures of 20 °C. To examine recovery, we used a paralysis recovery assay (see Materials and Methods) in which flies were held at 18 °C, rapidly paralyzed by shifting to 32 °C for 2 min, followed by recovery at 20 °C. Using this approach we found that *Ppt1* mutations had no effect on recovery rates of *shibire* mutant flies (**Fig. 1C**).

Synaptic development appears normal in *Ppt1* mutants

The paralysis assays further confirmed a role for *Ppt1* in synaptic vesicle cycling. Several genes known to play a role in this process also play a role in the structural development of the synapse.[33] To determine if there were structural abnormalities associated with these mutants, we examined synaptic development in *Ppt1* third instar larvae. Staining of the *Ppt1* deficiency mutant larval neuromuscular junctions showed no gross morphological changes, and bouton number (100 +/− 7.02), as shown by anti-synaptotagmin staining, was not significantly altered as compared with wild-type controls (116 +/− 4.60; $p = 0.11$, Nonparametric Mann Whitney U Test) (**Fig. 2A and B**).

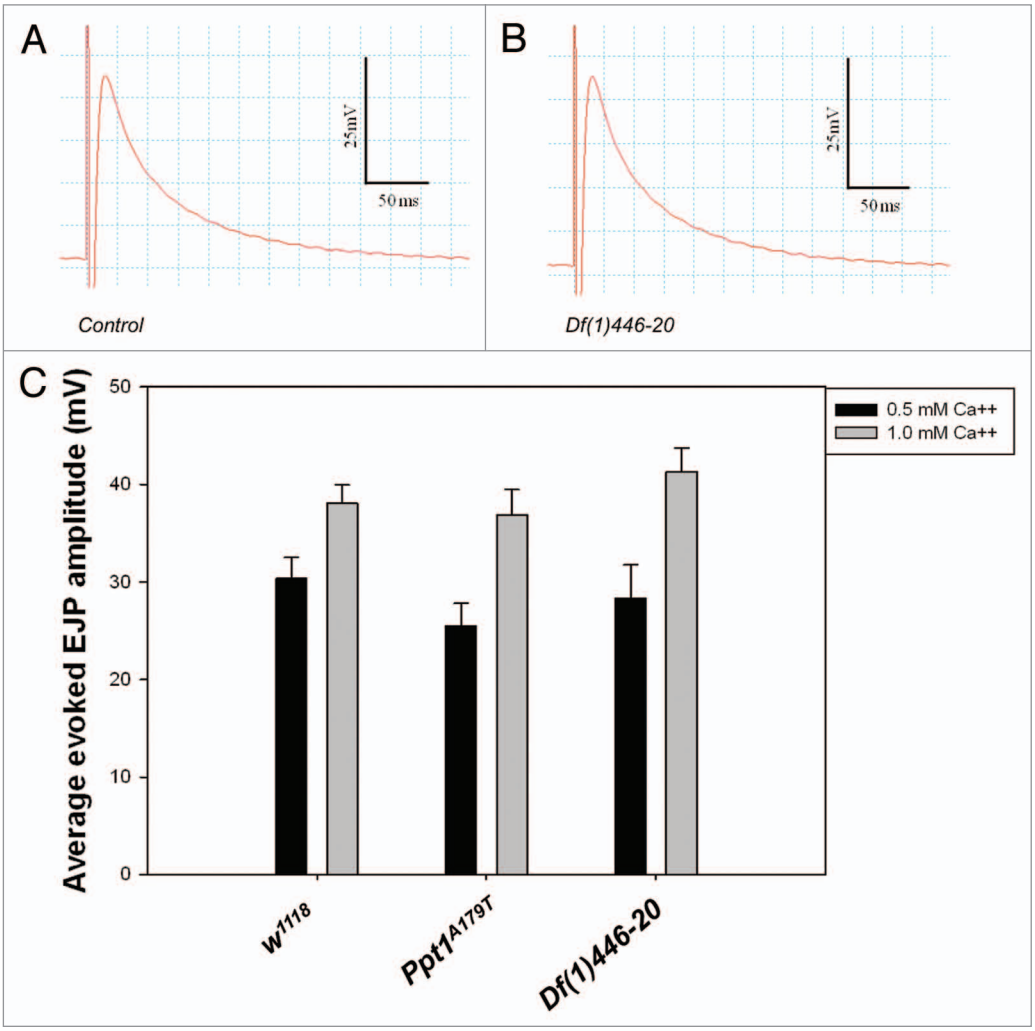

Figure 4. *Ppt1* mutations do not alter evoked EJPs. Representative traces of spontaneous miniature EJPs in muscle 6 of w^{1118} control larvae (**A**) and *Df(1)446–20* larvae (**B**). (**C**) A graph showing evoked EJP amplitudes in 1.0 and 0.5 mM Ca^{2+}. In 1.0 mM Ca^{2+}, average evoked EJP amplitudes were not significantly different in muscles from w^{1118} control (n = 20), $Ppt1^{A179T}$(n = 16), or *Df(1)446–20* (n = 20) larvae (p > 0.05). In 0.5mM Ca^{2+}, the average evoked EJP amplitudes were also not significantly different between the 3 genotypes (p > 0.05; w^{1118} control [n = 17], $Ppt1^{A179T}$ [n = 16], or *Df(1)446–20* [n = 16]).

***Ppt1* mutations affect mini EJP frequency but not amplitude**

Given the absence of significantly altered synaptic morphology, we asked whether *Ppt1* mutations impacted synaptic transmission by examining spontaneous neurotransmitter release at the 3rd instar larval neuromuscular junction. Motor neuron synapses onto muscle 6 of the body wall provide a well-characterized electrophysiological system that can be used to directly examine whether mutations of *Ppt1* elicit a change in pre- or post-synaptic function. To begin our characterization of possible NMJ phenotypes, we analyzed the frequency and amplitude of spontaneous miniature excitatory junction potentials (mini EJPs). Work at the frog neuromuscular junction has shown that changes in presynaptic function result in changes in the frequency of miniature synaptic potentials, whereas postsynaptic changes lead to changes in the amplitude of these events.[34] None of the mutants showed any significant difference from wild-type flies in the amplitude of observed minis (**Fig. 3A–B**). Average mini EJP amplitudes were 1.13 +/− 0.16 mV for w^{1118} wild-type flies (n = 16 cells from 13 larvae), 1.29 +/− 0.28 mV for $Ppt1^{A179T}$ point mutants (n = 10 cells, 9 larvae), 1.09 +/− 0.11 mV for $Ppt1^{S77F}$ point mutants (n = 20 cells, 18 larvae), 0.82 +/− 0.09 mV for *Df(1)446–20* mutants (n = 17 cells, 16 larvae), and 0.93 +/− 0.15 mV for *Df(1)446–20;elav-Gal4/UAS-Ppt1* rescue flies (n = 10 cells, 5 larvae). The average resting potentials also did not differ significantly between the genotypes (Vm = -65.44 +/− 1.23 mV, -63.1 +/− 1.02 mV, -64.6 +/− 1.12 mV, -65.35 +/− 1.24 mV, and -65.2 +/− 1.29 mv, for w^{1118}, $Ppt1^{A179T}$, $Ppt1^{S77}$, *Df(1)446–20* and *Df(1)446–20;elav-Gal4/UAS-Ppt1* rescue flies, respectively). Since the post-synaptic receptor is what determines the amplitude of the post-synaptic response, the lack of significant difference in amplitude implies that there is probably no defect in larval post-synaptic function in these mutants.[35]

The frequency of miniature events is dictated by the pre-synaptic function of synaptic release.[34] We observed increased mini EJP frequency in the *Df(1)446–20* mutants

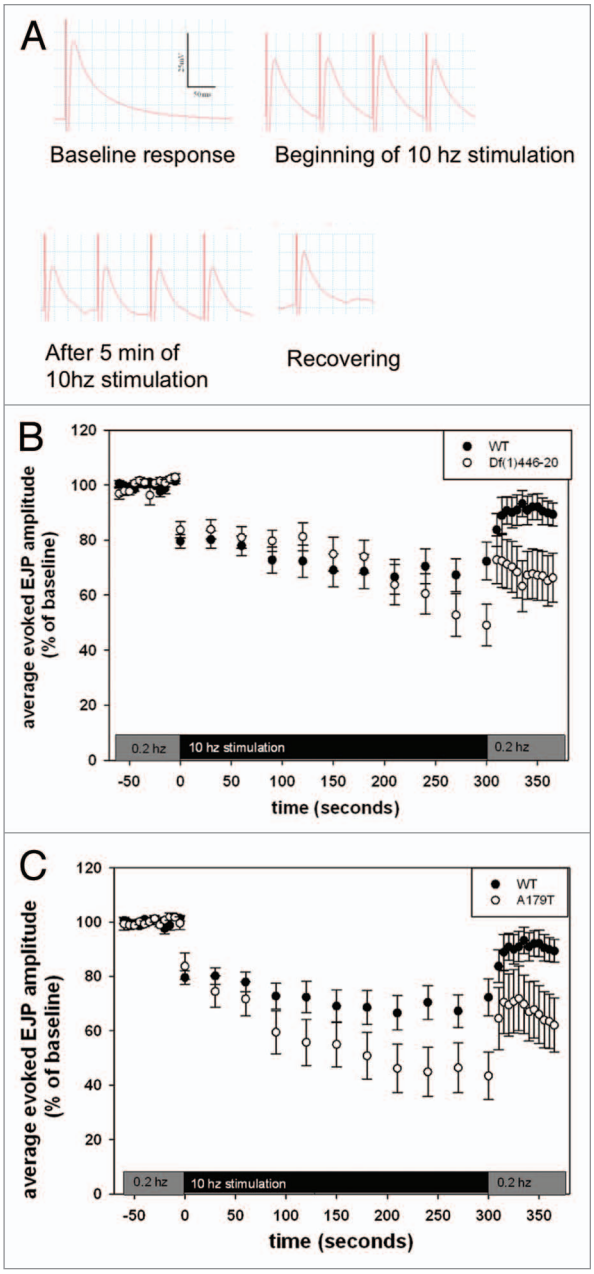

Figure 5. Repetitive stimulation of *Ppt1*^{A179T} and *Df(1)446–20* motor neurons reveals more rapid vesicle depletion and slower vesicle recycling. (**A**) Evoked EJPs in muscle cells of *w*^{1118} larvae before, at the start, and at the end of 10 Hz repetitive stimulation, and during the recovery phase following 10 Hz stimulation. (**B**) and (**C**) Evoked EJP amplitudes normalized to the pre-10 Hz- stimulation size, in W1118 and Df(1) 446–20 larvae (**B**) or W1118 and (*Ppt1*^{A179T}) larvae. Before the 10 Hz stimulation the EJP amplitudes did not differ significantly. At the end of the 10 Hz stimulation, and 60 s after recovery, EJPs in the mutant larvae were significantly different from wild type (* = p < 0.05, repeated measures ANOVA; *w*^{1118}, n = 20; *Ppt1*^{A179T}, n = 16; *Df(1)446–20*, n = 20).

(p < 0.05, 1-way ANOVA), suggesting that this mutation did in fact elicit a change in pre-synaptic function at the neuromuscular junction (**Fig. 3A and C**). Average mini EJP frequencies were 3.8 +/− 0.35 EJPs per second for *w*^{1118} wild-type flies (n = 16), 4.2 +/− 0.50 events per second for *Ppt1*^{A179T} point mutants (n = 10), 3.0 +/− 0.56 events per second for *Ppt1*^{S77F} point mutants (n = 20), 5.6 +/− 0.84 events per second for *Df(1)446–20* mutants (n = 17), and 5.4 +/− 0.73 events per second for *Df(1)446–20*;elav/+ (n = 7 cells). We observed no difference in mini EJP frequency between wild-type *w*^{1118} flies and rescued flies of the genotype *Df(1)446–20;elav-Gal4/UAS-Ppt1* (**Fig. 3C**). *Df(1)446–20;elav-Gal4/UAS-Ppt1* flies had an average mini EJP frequency of 3.2 +/− 0.37 events per second (n = 10), which was not significantly different from 3.8 +/− 0.35 events per second for *w*^{1118} flies (p > 0.05, one-way ANOVA). The rescue of the increased mini-EJP frequency by expression of Ppt1 pre-synaptically demonstrates that loss of pre-synaptic *Ppt1* function is responsible for the altered synaptic function.

***Ppt1* mutations show enhanced vesicle depletion and impaired vesicle recycling**

To determine whether Ppt1 is involved in calcium-mediated synaptic transmission, we stimulated the motor neurons innervating the body wall muscles and recorded evoked EJPs in muscle 6. The evoked EJPs recorded in 1.0 or 0.5 mM Ca^{2+} in *Ppt1*^{A179T} and *Df(1)446–20* larvae were not significantly different from those produced in *w*^{1118} wild-type muscle (**Fig. 4A–B**). In 1 mM Ca^{2+} the evoked EJP amplitudes were 38.05 ± 1.89 mV for *w*^{1118} wild-type larvae (n = 20), 36.89 ± 2.57 mV for the *Ppt1*^{A179T} point mutant (n = 16), 36.14 ± 4.44 mV for the *Ppt1*^{S77F} point mutant (n = 14, not shown), and 41.32 ± 2.43 mV for *Df(1)446–20* deficient mutants (n = 20) (**Fig. 4C**). Evoked EJPs were significantly smaller in 0.5 mM Ca^{2+}, but not different across genotypes (30.33 +/− 2.17 mV (n = 17) 25.47 +/− 2.33 mV (n = 16), and 28.32 +/− 3.42 mV (n = 16) for *w*^{1118}, *Ppt1*^{A179T}, and *Df(1)446–20* larvae, respectively (**Fig. 4C**). Thus, it appears that Ppt1 is not required for stimulus-evoked exocytosis under the conditions tested.

To examine whether Ppt1 or its substrates play a role in controlling vesicle depletion and recycling during and after high-frequency stimulation, we stimulated the motor nerve at 0.2 Hz, and then repetitively at 10 Hz for 5 min. We then measured the amplitude of the evoked EJPs throughout the baseline and stimulation periods (**Fig. 5A**). We followed this pattern with stimulation at 0.2 Hz to investigate potential differences in the recovery from the repetitive stimulation. As mentioned above, the baseline EJPs were not significantly different across genotypes (p > 0.05, repeated measures ANOVA), and therefore, we normalized the data to the size of the baseline responses. Repetitive stimulation leads to the rapid loss of synaptic vesicles from the readily releasable pool, followed by loss from the recycling pool; with more intense stimulation or in compromised synapses, vesicles are recruited from the reserve pool.[36,37] Evoked EJPs in the *Df(1)446–20* larvae showed a gradual decline in evoked EJP amplitude during the 10 Hz stimulation, while EJPs in the *w*^{1118} wild-type larvae declined slightly less throughout the repetitive stimulation (**Fig. 5B**). The percentage change in evoked EJP amplitude of *Df(1)446–20* deficient mutants was not significantly different from those in *w*^{1118} wild-type larvae at any point during the 10 Hz stimulation, except at 300 s, i.e., the end of high frequency stimulation (p < 0.05; **Fig. 5**). Evoked EJPs in *Ppt1*^{A179T} point mutants initially declined in a similar fashion to

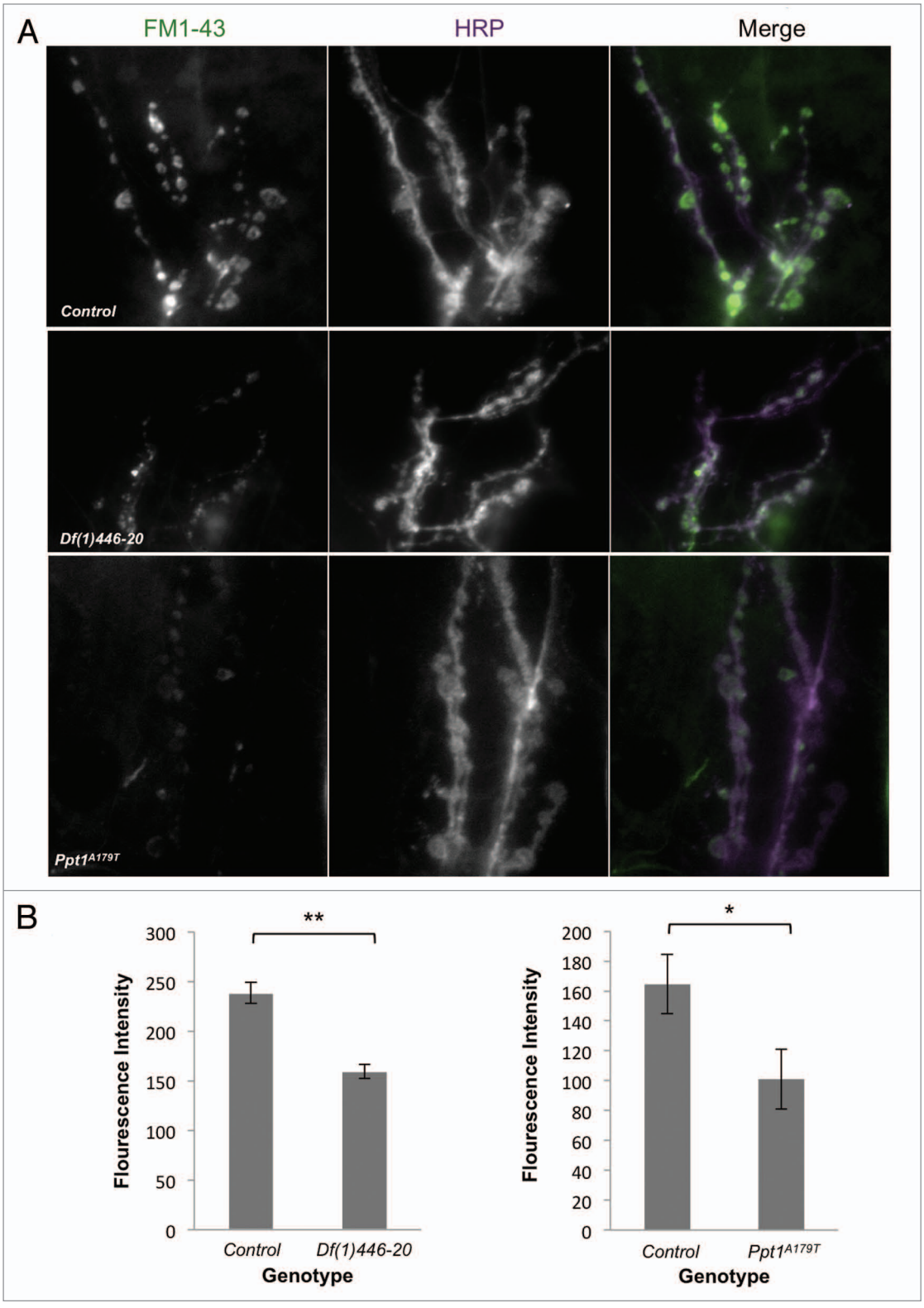

Figure 6. *Ppt1* mutant synapses have reduced FM1–43 uptake. (**A**) Images of control and *Ppt1* mutant (*Df(1)446–20* and *Ppt1*^{A179T}) third instar NMJs from muscle 6/7 in abdominal segment A2. Control larvae show increased levels of FM1–43 fluorescence as compared with synapses from *Ppt1* mutant larvae after 1 min stimulation with 90 mM K^+. Each panel is a single slice from a confocal z-stack showing the green channel (FM-143), the red channel (HRP), and the merged imaged. (**B**) Graphs showing the quantification of the average (average ± SE). FM1–43 fluorescence intensity for independent experiments that compared *Df(1)446–20* and *Ppt1*^{A179T} synapses to control larvae. *Df(1)446–20* showed a significant reduction in fluorescence as compared with control synapses (*control:* 238.46 ± 10.75, n = 152 boutons, 4 larvae vs. *Df(1)446–20*: 159.22 ± 6.99, n = 229 boutons, 4 larvae; nested ANOVA, $F_{(1,6)} = 15.79$; **, $p < 0.0001$). *Ppt1*^{A179T} also showed a significant reduction in fluorescence as compared with control synapses (*control:* 164.69 ± 15.31, n = 144 boutons, 4 larvae vs. *Ppt1*^{A179T}: 101.02 ± 11.13, n = 208 boutons, 4 larvae; nested ANOVA, $F_{(1,6)} = 8.99$; *, $p < 0.003$).

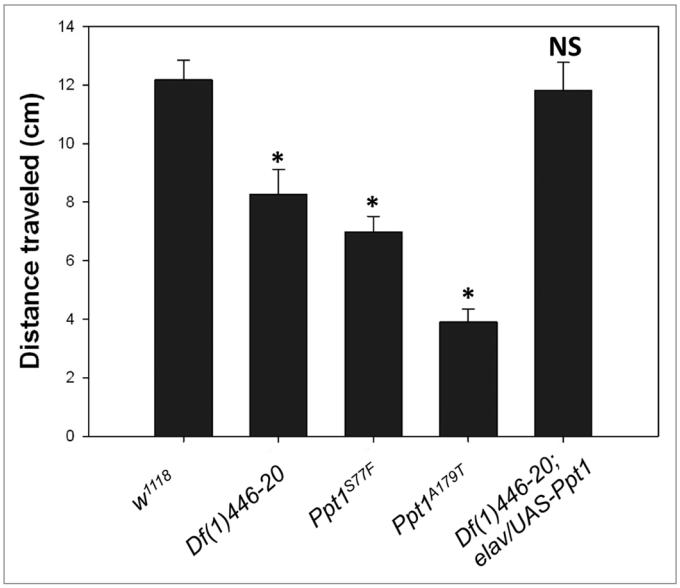

Figure 7. *Ppt1* mutant larvae have locomotion defects. A graphical representation of locomotor assay results for control (w^{1118}, n = 38), *Ppt1* point mutants ($Ppt1^{S77F}$, n = 29 and $Ppt1^{A179T}$, n = 20), *Ppt1*-deficient mutant (*Df(1)446–20*, n = 29) and *Ppt1* rescued mutant *Drosophila* larvae (*Df(1)446–20*; *elav-Gal4/UAS:Ppt1*, n = 26). Control larvae had a significantly greater path length than *Ppt1*-deficient and *Ppt1* point mutants (*, $p < 0.05$). Expressing *Ppt1* in the nervous system with *elav-Gal4* produced a path length that did not differ significantly from wild type (NS, $p > 0.05$).

those in wild-type, but continued to decline with the repetitive stimulation. After 180 s of 10 Hz stimulation the EJPs were noticeably smaller than the w^{1118} wild-type EJPs. The evoked EJP amplitudes were significantly different from those in w^{1118} for the last full minute of 10 Hz stimulation ($p < 0.05$; **Fig. 5C**).

To investigate whether synapses in these mutants can recover from the synaptic depression elicited by 10 Hz stimulation, EJPs elicited by the baseline stimulation frequency (0.2 Hz) were monitored for an additional minute or longer. The level of recovery was significantly lower in *Df(1)446–20* mutants compared with w^{1118} ($p < 0.05$; repeated measures ANOVA). At w^{1118} synapses, EJPs recovered to 89.33 ± 4.14% of the baseline responses 60 s after returning to the 0.2 Hz stimulation, whereas in *Df(1)446–20* synapses the EJPs were only 66.3 ± 8.95% of baseline (**Fig. 5B**). Recovery of EJP amplitudes at $Ppt1^{A179T}$ synapses was similarly compromised, reaching 62.09 ± 9.9% of the baseline responses, which, like the *Df(1)446–20* responses, were significantly different from the w^{1118} responses ($p < 0.5$; **Fig. 5C**). Thus, w^{1118} synapses have significantly greater vesicle recovery than those in either of the mutant genotypes.

***Ppt1* mutations reduce endocytosis as measured by FM1–43 uptake**

To assess more directly the impact of *Ppt1* mutations on vesicle cycling and endocytosis, we used the fluorescent endocytic tracer FM1–43X to measure synaptic endocytosis at third instar NMJs of control and *Ppt1* mutant larvae. Flourescence of FM1–43X, a fixable version of FM1–43, is not detectable when in an aqueous environment, but its quantum yield increases significantly after it is endocytosed at *Drosophila* synapses and interacts with the vesicle membrane.[38] The uptake of the tracer and subsequent fluorescence therefore allows for a quantitative measurement of vesicle cycling at the NMJ. As shown in **Figure 6A**, when control larvae were stimulated for 1 min with 90mM K^+ there was a significant uptake of the dye, as indicated by the bright fluorescent signal in individual boutons. This particular stimulation protocol preferentially labels the exo-endo cycling pool of vesicles at the synapse.[38] When a similar protocol was used to stimulate endocytosis in *Ppt1* mutant larvae, both *Df(1)446–20* and $Ppt1^{A179T}$ synapses showed a significant reduction (~40%) in tracer uptake, indicating that there is a defect in endocytosis at the NMJ (**Fig. 6B**).

Larval locomotion is impaired in *Ppt1* mutants

Examining locomotion in adult or larvae has proven to be a useful way to connect behavior and synaptic function.[39] In addition, the paralysis behavioral assays discussed above were performed in adults in which previous work has demonstrated the accumulation of abnormal storage material. Storage material does not yet appear in the larval nervous system and we wanted to determine if our cellular phenotypes also impacted obseeved behavior in the absence of inclusions. Thus, to complement our larval physiology and uptake data, we performed a locomotor path-length assay to examine potential behavioral effects caused by the loss of *Ppt1* function in wandering third instar larvae. After allowing larvae to crawl on agarose plates for five minutes, both the *Ppt1*-deficient (*Df(1)446–20*) as well as the 2 *Ppt1* point mutants ($Ppt1^{A179T}$ and $Ppt1^{S77F}$) exhibited significantly shorter average path lengths compared with those of wild-type larvae (w^{1118}; $p < 0.05$; **Fig. 7**). Wild-type *Drosophila* had an average path length of 12.16 ± 0.68 cm (n = 38; **Fig. 7**). The average path length was 8.25 ± 0.87 cm (n = 29), 6.96 ± 0.55 cm (n = 29), and 3.90 ± 0.45 cm (n = 20) for *Df(1)446–20*, $Ppt1^{S77F}$, and $Ppt1^{A179T}$, respectively (**Fig. 7**). When the *Ppt1* mutation was rescued using *elav-Gal4* (*Df(1)446–20; UAS-Ppt1, elav-Gal4*), the average path length traveled was 11.81 ± 0.96 (n = 26; **Fig. 1**), which is not significantly different from wild type. ($p > 0.05$). These results suggest that the reduced path-lengths we observed were caused solely by the loss of Ppt1 activity in the larval nervous system and may be attributable to reduced motor function.

Discussion

The work described here extends our understanding of Ppt1 function in the *Drosophila* nervous system. In particular, we have shown that *Ppt1* loss-of-function mutations show an increased frequency of mini EJPs, defects in vesicle cycling during and following repetitive stimulation, and a decreased rate of FM1–43 endocytosis. These phenotypes suggest a role for Ppt1 at the neuromuscular junction that is further supported by the locomotion defects observed in mutant larvae and the genetic interactions between *Ppt1* mutations and temperature sensitive *shibire* alleles. The more direct functional connections to synaptic vesicle recycling described here are built upon previous data from *Ppt1* genetic modifier screens that identified enhancer/suppressor loci such as *endophilin A*, *dynamin*, and *synaptotagmin*.[22,23]

Alterations in motor function

Our observation that the locomotion defects in the *Ppt1* mutants could be rescued by reintroduction of neural wild type Ppt1 activity suggests that loss of Ppt1 in the nervous system was the primary cause for the decrease in locomotor behavior. These results agree with those of Macauley et al.,[40] who found that PPT1$^{-/-}$ mice exhibit a decline in motor functioning as measured by performance on a rotorod. Whereas the locomotor defects in PPT1$^{-/-}$ mice coincide with cerebellar neuronal loss, however, the locomotor defects observed in *Drosophila* larvae occur before intracellular inclusions are observed in the nervous system.[17] It is unclear whether the motor dysfunction in human INCL patients precedes or requires neuronal loss, although some synaptic phenotypes are observed in the absence of typical NCL pathology in cultured mouse cortical neurons, indicating that important neuronal processes are disrupted early in the disease process.[25] This is consistent with the work presented here, suggesting that the larval synaptic phenotypes we describe in the fly are very relevant to NCL disease etiology.

Alterations in exo- and endocytosis

Our findings elucidate several presynaptic modifications that are connected to the loss of Ppt1 function. The increase in miniature EJPs in the Ppt1-deficient synapses suggests an increase in spontaneous fusion of synaptic vesicles with the presynaptic membrane, compared with their wild type and point-mutant counterparts, all of which had similar mEJP frequencies. The reversibility of the Ppt1 deficiency by pre-synaptic rescue of the gene, and the lack of change in the mini EJP amplitude in the Ppt1-deficient larvae, demonstrates that the effects at the post-synapse are likely to be minimal.[34] These results are also consistent with previous studies identifying potential pre-synaptic substrates of Ppt1 and its possible localization, which do not point to an interaction of Ppt1 with receptors or other post-synaptic targets.[26,41] Instead, most of the potential neuronal substrates, such as dynamin, SNAP25, CSP, VAMP2, syntaxin 1, SYTI, and GAD65, are pre-synaptic and control synaptic vesicle cycling. It is curious that the point mutation in the Ppt1 active site (*Ppt1^{A179T}*) failed to modify mini EJP frequency. It is possible that the substrates involved in spontaneous vesicle fusions can still interact with this mutant enzyme, and/or there is some residual thioesterase activity in the point mutant, whereas complete absence of the enzyme eliminates a "brake" on spontaneous release.

Although the Ppt1-deficiency affected spontaneous release of glutamate at these synapses, the loss of Ppt1 does not appear to affect stimulus-evoked release, even at reduced calcium concentrations. This is consistent with observations of excitatory postsynaptic potentials in hippocampal pyramidal neurons of acute brain slices and cortical neuron cultures prepared from Ppt1-knockout mice.[24,25] This suggests that at low stimulus frequencies, calcium-evoked glutamate release from Ppt1-deficient neurons is intact. At higher (e.g., 10 Hz) stimulus frequencies, as tested here and by Virmani et al.,[25] *Ppt1*-mutant nerve terminals show initial rates of depression, during the first 10 s of stimulation, that are similar to those of wild-type nerve terminals. With prolonged 10 Hz stimulation, however, the *Ppt1* mutant (*Df(1)* or *Ppt1^{A179T}*) nerve terminals show significantly more depression than their wild-type counterparts, perhaps due to an enhanced depletion of synaptic vesicles. Though we have not yet examined synaptic vesicle numbers in *Drosophila Ppt1*-mutant nerve terminals, several groups have shown that loss of PPT1 in mouse cortical neurons in vitro results in a decline in the size of the readily releasable synaptic vesicle pool as well as the total vesicle pool.[25,26] Such changes in vesicle number are likely due to reductions in endocytosis, perhaps due to alteration in the function of dynamin and other palmitoylated presynaptic proteins. Indeed, consistent with in vitro mouse results, we have observed a significantly reduced ability of *Ppt1* loss-of-function nerve terminals to recover from repetitive stimulation, as well as reductions in in vivo endocytosis measured by FM1–43 uptake (**Fig. 6**).

These observations provide a mechanistic explanation for our experimental results demonstrating a genetic enhancement of *shi* temperature sensitive mutant paralytic phenotypes and *Ppt1* loss-of-function point mutations. This confirms our previous work showing gain-of-function genetic interactions between these 2 loci and electron microscopic analysis of *Ppt1^{A179T}* garland cells that revealed ultrastructural defects in endocytic processes similar to those observed in *dynamin* mutants.[23] Taken together, these data support a direct role for Ppt1 and de-palmitoylation in modulating endocytosis. A reduced synaptic vesicle pool, produced by disruption of dynamin function and reduced synaptic vesicle recycling, could account for the genetic interaction between *Ppt1* and *shi* temperature sensitive paralysis mutants. Alternatively, dysregulation of exocytosis could also influence paralysis rates. These 2 models are not mutually exclusive given the effects we have shown on both processes in this paper and for the fact that several proteins involved in both the exo- and endocytic portions of the cycle are likely palmitoylated. Future experiments that closely examine synaptic vesicle populations in these nerve terminals will provide further support of that hypothesis.

Allele behavior

The behavior of the point mutations in relation to the deficiency differed depending on the experimental context. For example, the frequency of mini-EJPs was altered in the *Df(1)* line but not in the *Ppt1^{A179}* line (**Fig. 3**). Conversely, evoked EJPs in the *Ppt1^{A179}* line seemed to fatigue more quickly with repetitive stimulation than evoked EJPs in the *Df(1)* line, whereas recovery from the repetitive stimulation was defective in both genotypes (**Fig. 4**). It is unclear why these differences in electrophysiological phenotype were observed in the different mutant lines, and why the locomotion phenotype was most severe in the *Ppt1^{A179}* mutants. The deficiency completely removes the coding region of *Ppt1* and thus represents the complete loss of Ppt1 function in the fly.[17] The Alanine to Threonine mutation (*Ppt1^{A179}*) is analogous to position 171 in the human protein and is located at the distal end of the substrate binding pocket. Human INCL mutations, V181M and E184K, are also located in this region and result in an almost complete loss (< 2%) of wild-type function.[42,43] The Serine to Phenylalanine mutation (*Ppt1^{S77F}*), analogous to Serine 69 in the human protein, is located outside of the active site and though there is no human INCL mutation at this residue, there

are 2 disease-causing mutations nearby (T75P and D79G) that cause a later-onset form of NCL.[42,43] While there is little enzyme activity associated with these point mutations in humans, there is some remaining immunoreactivity in patient cell lines, demonstrating that Ppt1 protein is still being made at reduced levels.[42] In the fly, the point mutants behave similarly to the *Df(1)* in an enzymatic assay, although any residual activity in the point mutants is likely outside the sensitivity of the assay.[17] Lifespan assays with heterozygous combinations of the point mutations and the *Df(1)* line suggest that there is some residual function of the enzyme indicating that the mutant proteins may be expressed at low levels with important functional consequences.[17] Finally, it is also possible that some genetic background differences between the point mutations and the *Df(1)* line may explain some of the variability. As a whole, regardless of genetic mutation, our work points directly to a role for Ppt1 function in synaptic exo- and endocytosis. It also suggests that the further study of individual point mutations, at the genetic and biochemical level, may reveal important mechanistic information about Ppt1's function during these important synaptic processes.

Connections to substrates

The synaptic phenotypes we report here are consistent with and expand upon published results from several groups working in mouse models.[25,26] The biochemical basis for these phenotypes is less clear. Although we currently lack optimal reagents, such as an effective *Drosophila* anti-Ppt1 antibody that will allow us to confirm a presynaptic localization of Ppt1, we can speculate that a small pool of endogenous Ppt1 is likely to be at the synapse in the fly as has been observed by one group in mouse tissue.[26,41] Even if Ppt1 is primarily lysosomal in *Drosophila* that does not preclude an indirect, although important, impact on synaptic function. The build-up of membrane-bound palmitoylated metabolites in Ppt1 deficient flies, similar to what is observed in humans, could directly interfere with the function of important palmitoylated synaptic proteins.[25,26]

SNAP-25 and CSP are especially attractive Ppt1 substrate candidates. SNAP-25 is palmitoylated, and this palmitoylation occurs simultaneous with and is necessary for membrane association.[44] A comparison of the synaptic phenotypes we characterized suggests that SNAP-25 is a Ppt1 substrate. Similar to *Df(1)446–20* larvae, temperature-sensitive *SNAP-25* (*SNAP-25^{ts})* larvae show increased mini-EJP frequency at 22 °C with no differences in mini-EJP amplitude.[45] The authors suggested that the *SNAP-25^{ts}* mutation may yield more fusion-ready SNARE complexes, thus increasing the frequency of vesicle fusion.[45] The phenocopy of this mutation by a null *Ppt1* mutation may be associated with a dysregulation of SNAP-25 palmitoylation, leading to an increase in membrane-associated, palmitoylated SNAP-25 following vesicle release. This might produce an increase in spontaneous fusion events, as exemplified by the increase in mini EJPs. This is supported by the recent observation of increased membrane sorting and retention of SNAP-25 and other presynaptic palmitoylated proteins in neurons of Ppt1-deficient mice or humans.[26] Future experiments will be needed to determine if depalmitoylation is necessary for SNAP-25 membrane dissociation and whether this event occurs concurrently with cessation of presynaptic neurotransmitter release.

Considering the recent implication of cysteine string protein (CSP) mutations (*DNAJC5)* in adult-onset NCL,[46-48] and the known palmitoylation of this presynaptic protein,[2,48] CSP is another candidate that likely has an altered function and localization in *Ppt1*-mutant *Drosophila* as well as INCL patients. In adult-onset NCL patients (also known as Kufs Disease), identified mutations in *CSP*α gene are found in the cysteine-string domain and are known to affect palmitoylation and its intracellular localization.[2,50] This leads to reductions in overall levels of CSPα and neurodegeneration,[47] and/or aggregation of the mutant CSPα monomers.[50] At a functional level, recent experiments using CSPα knockout mice have shown an intimate connection between CSPα, dynamin 1, SNAP-25 and exo/endocytic coupling, elucidating a direct molecular connection for CSP to synaptic vesicle pool maintenance.[51,52]

In *Drosophila,* palmitoylation of CSP and SNAP25 is clearly necessary for their proper trafficking within the cell, as shown by the consequences of mutations in the neuronal palmitoyl acyl transferase, Hip14.[27,28,53] Whether depalmitoylation by protein thioesterases also influences trafficking and functioning of synaptic proteins to and from the nerve terminals is unknown, but likely, particularly for the peripheral membrane proteins that associate with the membrane using palmitoyl moieties. The role of palmitoylation for transmembrane protein localization and function is even less clear; however, the observation that changes in neuronal activity can influence the palmitoylation of proteins like synaptotagmin 1 and PSD95 suggests that this highly dynamic, reversible process may be critical to the functions of proteins involved in synaptic transmission.[54] In the case of repetitive stimulation for long durations, our results suggest that depalmitoylation is necessary for the recycling of vesicles needed to replenish the readily releasable store of vesicles.

The evidence we have presented would suggest that, rather than a general alteration in palmitoylation, Ppt1 may modulate critical pre-synaptic components, such as CSP, SNAP25, and Dynamin, that are essential for efficient exo/endocytic coupling at the synapse. Taken as a whole, these data move our understanding of the disease process forward by demonstrating the importance of palmitoylation as a regulatory mechanism in synaptic processes and implicates particular proteins in the etiology of INCL. Considering the numerous genetic tools available in *Drosophila*, and the ability to look at genetic interactions between *Ppt1* mutations and mutations in potential substrate proteins, this species will likely continue to serve as a viable model system for understanding INCL, other NCL diseases, and general neurodegenerative processes.

Materials and Methods

***Drosophila* strains and genetics**

Fly stocks were maintained on standard medium at 25 °C, except *shi-Ppt1* recombinant stocks, which were maintained at 18 °C. *Df(1)446–20* (FBal0150942) is a small deletion that completely removes the *ppt1* locus and 3 other loci

(*CG11294, CG1795, and CG11285;* Glaser et al., 2003). The neuronal-specific inclusions observed in this deficiency line are completely rescued by *elav-Gal4 (*FBst0038399*)* driven expression of a *UAS:Ppt1* (FBal0193173) transgene.[17] The *Ppt1*^{A179T} (FBal0193174) and *Ppt1*^{S77F} (FBal0193175) point mutations are loss-of-function alleles that were created and maintained on an isogenic background for these experiments.[17] The neuronal specific inclusions observed in these point mutants are also completely rescued by *elav-Gal4* driven expression of a *UAS:Ppt1* transgene.[17] *shi*^{1} (FBst0304950) and *shi*^{2} (FBst0305416) were obtained from the Bloomington Drosophila Stock Center (Bloomington, IN). The *UAS:Ppt1* transgenic lines were previously described.[18] All other lines used in this study were obtained from Bloomington.

Locomotor assays

Locomotor assays were performed to examine potential differences in motor behavior of the PPT1 mutants compared with wild-type *Drosophila*; 5 genotypes were investigated (*w*^{1118}, *Df(1)446–20*, *Ppt1*^{S77F}, *Ppt1*^{A179T}, and *Df(1)446–20; UAS-Ppt1, elav-Gal4*). Third instar larvae were placed on 1% agarose plates (9 cm petri dishes) for 5 min at room temperature (23 °C) while their paths were traced on the petri dish lids.[55,56] ImageJ was used to measure the path lengths, and differences in path length were compared using 2-way ANOVA.

Miniature and evoked excitatory junction potential (EJP) recording

Third instar larvae were pinned to a Sylgard™ substrate and dissected in Ca^{2+}-free HL3 (70 mM NaCl, 5 mM KCl, 20 mM $MgCl_2 \cdot 6H_20$, 10 mM $NaHCO_3$, 5 mM D^+ Trehalose dihydrate, 115 mM Sucrose, and 5 mM Hepes acid)[57] to expose the body wall muscles. The motor nerves were cut near their attachment to the ventral nerve cord to prevent the generation of action potentials in motor axons from the CNS. Before recording, the Ca^{2+} free bath was exchanged three times with 1 mM or 0.5 mM Ca^{2+}-containing HL3 media at room temperature (23 °C). Intracellular recording electrodes (resistance 10–30 MΩ) were filled with 3 M KCl and placed in muscle fiber 6 in abdominal segment 3 or 4, and a reference electrode was placed in the bath. Signals were monitored with a Dagan IX1 amplifier in intracellular mode, digitized using a Powerlab 2/25 (ADInstruments) and displayed in Chart5 for Windows (2007). In muscle fibers with a resting membrane potential of at least -60 mV, mini EJPs were recorded for a minimum of 3 min, and their amplitudes and frequencies were analyzed using Chart 5 for Windows. Mini EJP amplitudes and frequencies were compared across genotypes using one-way ANOVAs. If a significant variation across genotypes was observed, the Fisher's PLSD post-hoc test was used to determine which groups differed significantly.

Evoked excitatory junction potentials and repetitive stimulation recordings

To elicit evoked EJPs, the segmental nerve was stimulated with a suction electrode filled with HL3, with 1 ms pulses generated at 0.05 Hz by an Isolator-II Stimulus Isolation Unit (Axon Instruments). Chart 5.5.6 for Windows was used to monitor the membrane potential as the recording electrode was placed in muscle 6. If the resting membrane potential was stable and more negative than -60 mV, the neuromuscular junction was stimulated at a frequency of 0.2 Hz for 1 min. Chart 5.5.6 was used for the stimulus protocol, data acquisition, and measurement of the amplitude of evoked EJPs. The baseline stimulation was followed by 5 min of repetitive 10 Hz stimulation, in attempt to measure the rate of vesicle depletion, and then followed by 1 min of 0.2 Hz stimulation to determine the rate of synaptic vesicle recovery. The amplitude of baseline evoked EJPs was measured every five seconds during the 0.2 Hz stimulation. During the 10 Hz stimulation, 10 consecutive EJPs were measured every 30 s. Each of the 10 responses was then averaged for a total of 11 average responses over 300 s. The recovery from repetitive stimulation was determined by measuring evoked EJPs every five seconds during the final 0.2 Hz stimulation period. Recordings were taken from at least 16 different larvae per genotype, and average evoked EJPs were compared using unpaired t-tests of unequal variance or repeated measures ANOVAs. All data are presented as average ± S.E.M., and the sample size (N) indicates the number of cells recorded in the same number of larvae.

Measuring endocytosis by FM1–43 uptake

FM1–43 uptake at third Instar NMJs was done according to Verstreken et al.[38] Briefly, third instar larvae were pinned to a Sylgard™ substrate and dissected in Ca^{2+}-free HL3 (110 mM NaCl, 5 mM KCl, 10 mM $MgCl_2$, 10 mM $NaHCO_3$, 5 mM trehalose, 30 mM Sucrose, and 5 mM Hepes) to expose the body wall muscles. The motor nerves were cut near their attachment to the ventral nerve cord to prevent the generation of action potentials in motor axons from the CNS. Labeling of exo-endo cycling synaptic vesicles was achieved by a 1 min KCl stimulation of the neurons in the presence of FM1–43X (Invitrogen). The HL3/FM1–43X labeling solution contained 90mM KCL and 4μM FM1–43X (25mM NaCl, 90 mM KCl, 10 mM $MgCl_2$, 10 mM $NaHCO_3$, 5 mM trehalose, 30 mM Sucrose, 5 mM Hepes, 1.5 mM $CaCl_2$, 4μM FM1–43X). After labeling, larvae were gently washed with Ca^{2+}-free HL3, fixed for 5 min with 4% Formaldehyde, unpinned and then incubated with Cy5 conjugated goat anti-HRP (Jackson ImmunoResearch Laboratories) to label the NMJ presynaptic membranes. Larvae were washed and mounted in Vectashield (Vector Labs) for confocal imaging. Neuromuscular junctions on muscle 6/7 in abdominal region A2 and A3 were immediately imaged on an Olympus IX71 Spinning Disc Confocal Microscope. Quantification of individual bouton (≥ 3μm) labeling intensity was performed as described in Verstreken et al. (2008) using the Olympus Slide Book analysis program. Uptake analysis was done on synapses from 8 wild-type larvae and 4 mutant larvae from 2 different mutant genotypes, *Df(1)446–20* and *Ppt1*^{A179T}. Statistical comparison of average bouton fluorescence between genotypes was done using a nested ANOVA of square root transformed data. All data are presented as average +/− SE, and the sample size (N) indicates the number of boutons analyzed for each genotype.

Generating *Ppt1-shibire* recombinants

Ppt1-shibire recombinant X-chromosomes were produced by crossing *Ppt1* females to *shibire* males to produce *Ppt1/shibire* female heterozygotes. Recombinant males were selected for in the F2 generation. To select recombinants for the *shi* alleles,

white-eyed males were collected and moved to a 29 °C incubator where *Ppt1/Y* males without the *shibire* gene did not paralyze. Paralyzed males were allowed to recover and stocks were produced from single males. To determine if the *shi* chromosome contained the *Ppt1* mutation, males from these stocks were then tested for the absence of Ppt1 activity using a fluorescent enzyme assay.[17]

Paralysis/recovery profiles

We performed paralysis assays to measure paralysis and recovery rates of 4 *Drosophila* lines (*shi*[1]; *shi*[2]; *shi*,[1] *Ppt1*^{A179T}; *shi*,[2] *Ppt1*^{S77F}) as previously described.[37] Briefly, the 4 genotypes were placed in vials with 10 flies each, and kept at 18 °C. Flies were temperature shifted to 27 °C in an incubator and paralysis was observed. After each 30s interval the number of non-paralyzed flies in each vial was recorded. Rescue experiments were done with a Y Chromosome, *Dp(1;Y)578*, carrying a duplicated piece of the *Ppt1* region that has been previously shown to rescue Ppt1-associated phenotypes.[17] We used the duplication to rescue this adult neural phenotype because UAS-driven expression of *Ppt1* in the nervous system has detrimental effects on adult lifespan and adult retinal development.[17,18] To observe recovery rates, flies of the appropriate genotypes were kept at 18 °C, and then heat shocked at 32 °C for 3 min to produce paralysis. The vials were moved to a 20 °C incubator for recovery observation. We recorded the number of recovered (non-paralyzed) flies in each vial at 30 s intervals.

NMJ immunohistochemistry

Four third-instar larvae were dissected to examine 8 individual muscle 6/7 neuromuscular junctions. To compare individual bouton numbers between wild-type and *Df(1)446–20* larvae, third-instar wandering larvae were collected from low-density cultures kept at 25 °C, dissected and fixed. Neuromuscular junctions were stained with anti-synaptotagmin rabbit polyclonal primary antibodies (Gift of Bellen H) and visualized with Alexa Fluor 488-conjugated goat anti-rabbit secondary antibody (Molecular Probes). Boutons were counted at muscle 6/7 in abdominal segment A2 (n = 9 A2 segments per genotype). All data are presented as average +/− SE. All confocal images were acquired on an Olympus IX71 Spinning Disc Confocal Microscope.

Disclosure of Potential Conflicts of Interest

No potential conflicts of interest were disclosed.

Acknowledgments

We would like to thank Jennifer Genova for technical assistance with the confocal microscopy and Steve Adolph for help with statistical analysis. This work was supported by National Institutes of Health grant #'s P20-RR16461 (Korey CA) and R15-HD052362 (Korey CA), The College of Charleston Undergraduate Research and Creative Activities Office, the Hirsch Foundation, and the Pomona College Summer Undergraduate Research Program.

References

1. Fukata Y, Fukata M. Protein palmitoylation in neuronal development and synaptic plasticity. Nat Rev Neurosci 2010; 11:161-75; PMID:20168314; http://dx.doi.org/10.1038/nrn2788
2. Greaves J, Chamberlain LH. Dual role of the cysteine-string domain in membrane binding and palmitoylation-dependent sorting of the molecular chaperone cysteine-string protein. Mol Biol Cell 2006; 17:4748-59; PMID:16943324; http://dx.doi.org/10.1091/mbc.E06-03-0183
3. Young FB, Butland SL, Sanders SS, Sutton LM, Hayden MR. Putting proteins in their place: palmitoylation in Huntington disease and other neuropsychiatric diseases. Prog Neurobiol 2012; 97:220-38; PMID:22155432; http://dx.doi.org/10.1016/j.pneurobio.2011.11.002
4. Vesa J, Hellsten E, Verkruyse LA, Camp LA, Rapola J, Santavuori P, Hofmann SL, Peltonen L. Mutations in the palmitoyl protein thioesterase gene causing infantile neuronal ceroid lipofuscinosis. Nature 1995; 376:584-7; PMID:7637805; http://dx.doi.org/10.1038/376584a0
5. Haltia M. The neuronal ceroid-lipofuscinoses: from past to present. Biochim Biophys Acta 2006; 1762:850-6; PMID:16908122; http://dx.doi.org/10.1016/j.bbadis.2006.06.010
6. Warrier V, Vieira M, Mole SE. Genetic basis and phenotypic correlations of the neuronal ceroid lipofusinoses. Biochim Biophys Acta 2013; 1832:1827-30; PMID:23542453; http://dx.doi.org/10.1016/j.bbadis.2013.03.017
7. Mitchison HM, Hofmann SL, Becerra CH, Munroe PB, Lake BD, Crow YJ, Stephenson JB, Williams RE, Hofman IL, Taschner PE, et al. Mutations in the palmitoyl-protein thioesterase gene (PPT; CLN1) causing juvenile neuronal ceroid lipofuscinosis with granular osmiophilic deposits. Hum Mol Genet 1998; 7:291-7; PMID:9425237; http://dx.doi.org/10.1093/hmg/7.2.291
8. van Diggelen OP, Thobois S, Tilikete C, Zabot MT, Keulemans JL, van Bunderen PA, Taschner PE, Losekoot M, Voznyi YV. Adult neuronal ceroid lipofuscinosis with palmitoyl-protein thioesterase deficiency: first adult-onset patients of a childhood disease. Ann Neurol 2001; 50:269-72; PMID:11506414; http://dx.doi.org/10.1002/ana.1103
9. Williams RE, Aberg L, Autti T, Goebel HH, Kohlschütter A, Lönnqvist T. Diagnosis of the neuronal ceroid lipofuscinoses: an update. Biochim Biophys Acta 2006; 1762:865-72; PMID:16930952; http://dx.doi.org/10.1016/j.bbadis.2006.07.001
10. Washbourne P. Greasing transmission: palmitoylation at the synapse. Neuron 2004; 44:901-2; PMID:15603731
11. Bond M, Holthaus SM, Tammen I, Tear G, Russell C. Use of model organisms for the study of neuronal ceroid lipofuscinosis. Biochim Biophys Acta 2013; 1832:1842-65; PMID:23338040; http://dx.doi.org/10.1016/j.bbadis.2013.01.009
12. Cauchi RJ, van den Heuvel M. The fly as a model for neurodegenerative diseases: is it worth the jump? Neurodegener Dis 2006; 3:338-56; PMID:17192723; http://dx.doi.org/10.1159/000097303
13. Jaiswal M, Sandoval H, Zhang K, Bayat V, Bellen HJ. Probing mechanisms that underlie human neurodegenerative diseases in Drosophila. Annu Rev Genet 2012; 46:371-96; PMID:22974305; http://dx.doi.org/10.1146/annurev-genet-110711-155456
14. Marsh JL, Thompson LM. Drosophila in the study of neurodegenerative disease. Neuron 2006; 52:169-78; PMID:17015234; http://dx.doi.org/10.1016/j.neuron.2006.09.025
15. Myllykangas L, Tyynelä J, Page-McCaw A, Rubin GM, Haltia MJ, Feany MB. Cathepsin D-deficient Drosophila recapitulate the key features of neuronal ceroid lipofuscinoses. Neurobiol Dis 2005; 19:194-9; PMID:15837574; http://dx.doi.org/10.1016/j.nbd.2004.12.019
16. Kuronen M, Talvitie M, Lehesjoki A-E, Myllykangas L. Genetic modifiers of degeneration in the cathepsin D deficient Drosophila model for neuronal ceroid lipofuscinosis. Neurobiol Dis 2009; 36:488-93; PMID:19761846; http://dx.doi.org/10.1016/j.nbd.2009.09.001
17. Hickey AJ, Chotkowski HL, Singh N, Ault JG, Korey CA, MacDonald ME, Glaser RL. Palmitoyl-protein thioesterase 1 deficiency in Drosophila melanogaster causes accumulation of abnormal storage material and reduced life span. Genetics 2006; 172:2379-90; PMID:16452138; http://dx.doi.org/10.1534/genetics.105.053306
18. Korey CA, MacDonald ME. An over-expression system for characterizing Ppt1 function in Drosophila. BMC Neurosci 2003; 4:30; PMID:14629778; http://dx.doi.org/10.1186/1471-2202-4-30
19. Tuxworth RI, Vivancos V, O'Hare MB, Tear G. Interactions between the juvenile Batten disease gene, CLN3, and the Notch and JNK signalling pathways. Hum Mol Genet 2009; 18:667-78; PMID:19028667; http://dx.doi.org/10.1093/hmg/ddn396
20. Tuxworth RI, Chen H, Vivancos V, Carvajal N, Huang X, Tear G. The Batten disease gene CLN3 is required for the response to oxidative stress. Hum Mol Genet 2011; 20:2037-47; PMID:21372148; http://dx.doi.org/10.1093/hmg/ddr088
21. Chu-LaGraff Q, Blanchette C, O'Hern P, Denefrio C. The Batten disease Palmitoyl Protein Thioesterase 1 gene regulates neural specification and axon connectivity during Drosophila embryonic development. PLoS One 2010; 5:e14402; PMID:21203506; http://dx.doi.org/10.1371/journal.pone.0014402
22. Buff H, Smith AC, Korey CA. Genetic modifiers of Drosophila palmitoyl-protein thioesterase 1-induced degeneration. Genetics 2007; 176:209-20; PMID:17409080; http://dx.doi.org/10.1534/genetics.106.067983

23. Saja S, Buff H, Smith AC, Williams TS, Korey CA. Identifying cellular pathways modulated by Drosophila palmitoyl-protein thioesterase 1 function. Neurobiol Dis 2010; 40:135-45; PMID:20206262; http://dx.doi.org/10.1016/j.nbd.2010.02.010
24. Ahtiainen L, Luiro K, Kauppi M, Tyynelä J, Kopra O, Jalanko A. Palmitoyl protein thioesterase 1 (PPT1) deficiency causes endocytic defects connected to abnormal saposin processing. Exp Cell Res 2006; 312:1540-53; PMID:16542649; http://dx.doi.org/10.1016/j.yexcr.2006.01.034
25. Virmani T, Gupta P, Liu X, Kavalali ET, Hofmann SL. Progressively reduced synaptic vesicle pool size in cultured neurons derived from neuronal ceroid lipofuscinosis-1 knockout mice. Neurobiol Dis 2005; 20:314-23; PMID:16242638; http://dx.doi.org/10.1016/j.nbd.2005.03.012
26. Kim SJ, Zhang Z, Sarkar C, Tsai PC, Lee YC, Dye L, Mukherjee AB. Palmitoyl protein thioesterase-1 deficiency impairs synaptic vesicle recycling at nerve terminals, contributing to neuropathology in humans and mice. J Clin Invest 2008; 118:3075-86; PMID:18704195; http://dx.doi.org/10.1172/JCI33482
27. Ohyama T, Verstreken P, Ly CV, Rosenmund T, Rajan A, Tien AC, Haueter C, Schulze KL, Bellen HJ. Huntingtin-interacting protein 14, a palmitoyl transferase required for exocytosis and targeting of CSP to synaptic vesicles. J Cell Biol 2007; 179:1481-96; PMID:18158335; http://dx.doi.org/10.1083/jcb.200710061
28. Stowers RS, Isacoff EY. Drosophila huntingtin-interacting protein 14 is a presynaptic protein required for photoreceptor synaptic transmission and expression of the palmitoylated proteins synaptosome-associated protein 25 and cysteine string protein. J Neurosci 2007; 27:12874-83; PMID:18032660; http://dx.doi.org/10.1523/JNEUROSCI.2464-07.2007
29. Siddiqi O, Benzer S. Neurophysiological defects in temperature-sensitive paralytic mutants of Drosophila melanogaster. Proc Natl Acad Sci U S A 1976; 73:3253-7; PMID:184469; http://dx.doi.org/10.1073/pnas.73.9.3253
30. Masur SK, Kim YT, Wu CF. Reversible inhibition of endocytosis in cultured neurons from the Drosophila temperature-sensitive mutant shibirets1. J Neurogenet 1990; 6:191-206; PMID:2113575; http://dx.doi.org/10.3109/01677069009107110
31. Zhang B. Genetic and molecular analysis of synaptic vesicle recycling in Drosophila. J Neurocytol 2003; 32:567-89; PMID:15034254; http://dx.doi.org/10.1023/B:NEUR.0000020611.44254.86
32. Narayanan R, Krämer H, Ramaswami M. Drosophila endosomal proteins hook and deep orange regulate synapse size but not synaptic vesicle recycling. J Neurobiol 2000; 45:05-119.
33. Dawson-Scully K, Lin Y, Imad M, Zhang J, Marin L, Horne JA, Meinertzhagen IA, Karunanithi S, Zinsmaier KE, Atwood HL. Morphological and functional effects of altered cysteine string protein at the Drosophila larval neuromuscular junction. Synapse 2007; 61:1-16; PMID:17068777; http://dx.doi.org/10.1002/syn.20335
34. Fatt P, Katz B. Spontaneous subthreshold activity at motor nerve endings. J Physiol 1952; 117:109-28; PMID:14946732
35. Katz B, Thesleff S. On the factors which determine the amplitude of the miniature end-plate potential. J Physiol 1957; 137:267-78; PMID:13449877
36. Rizzoli SO, Betz WJ. Synaptic vesicle pools. Nat Rev Neurosci 2005; 6:57-69; PMID:15611727; http://dx.doi.org/10.1038/nrn1583
37. Delgado R, Maureira C, Oliva C, Kidokoro Y, Labarca P. Size of vesicle pools, rates of mobilization, and recycling at neuromuscular synapses of a Drosophila mutant, shibire. Neuron 2000; 28:941-53; PMID:11163278; http://dx.doi.org/10.1016/S0896-6273(00)00165-3
38. Verstreken P, Ohyama T, Bellen HJ. FM1-43 Labeling of Synapic Vesicle Pools at the Drosophila Neuromuscular Junction. In A. Ivanov, ed. Exocytosis and Endocytosis. Totowa, NJ: Humana Press. 2008:349-369.
39. Feiguin F, Godena VK, Romano G, D'Ambrogio A, Klima R, Baralle FE. Depletion of TDP-43 affects Drosophila motoneurons terminal synapsis and locomotive behavior. FEBS Lett 2009; 583:1586-92; PMID:19379745; http://dx.doi.org/10.1016/j.febslet.2009.04.019
40. Macauley SL, Wozniak DF, Kielar C, Tan Y, Cooper JD, Sands MS. Cerebellar pathology and motor deficits in the palmitoyl protein thioesterase 1-deficient mouse. Exp Neurol 2009; 217:124-35; PMID:19416667; http://dx.doi.org/10.1016/j.expneurol.2009.01.022
41. Lehtovirta M, Kyttälä A, Eskelinen EL, Hess M, Heinonen O, Jalanko A. Palmitoyl protein thioesterase (PPT) localizes into synaptosomes and synaptic vesicles in neurons: implications for infantile neuronal ceroid lipofuscinosis (INCL). Hum Mol Genet 2001; 10:69-75; PMID:11136716; http://dx.doi.org/10.1093/hmg/10.1.69
42. Das AK, Lu JY, Hofmann SL. Biochemical analysis of mutations in palmitoyl-protein thioesterase causing infantile and late-onset forms of neuronal ceroid lipofuscinosis. Hum Mol Genet 2001; 10:1431-9; PMID:11440996; http://dx.doi.org/10.1093/hmg/10.13.1431
43. Ohno K, Saito S, Sugawara K, Suzuki T, Togawa T, Sakuraba H. Structural basis of neuronal ceroid lipofuscinosis 1. Brain Dev 2010; 32:524-30; PMID:19793631; http://dx.doi.org/10.1016/j.braindev.2009.08.010
44. Gonzalo S, Linder ME. SNAP-25 palmitoylation and plasma membrane targeting require a functional secretory pathway. Mol Biol Cell 1998; 9:585-97; PMID:9487128; http://dx.doi.org/10.1091/mbc.9.3.585
45. Rao SS, Stewart BA, Rivlin PK, Vilinsky I, Watson BO, Lang C, Boulianne G, Salpeter MM, Deitcher DL. Two distinct effects on neurotransmission in a temperature-sensitive SNAP-25 mutant. EMBO J 2001; 20:6761-71; PMID:11726512; http://dx.doi.org/10.1093/emboj/20.23.6761
46. Benitez BA, Alvarado D, Cai Y, Mayo K, Chakraverty S, Norton J, Morris JC, Sands MS, Goate A, Cruchaga C. Exome-sequencing confirms DNAJC5 mutations as cause of adult neuronal ceroid-lipofuscinosis. PLoS One 2011; 6:e26741; PMID:22073189; http://dx.doi.org/10.1371/journal.pone.0026741
47. Nosková L, Stránecký V, Hartmannová H, Pristoupilová A, Barešová V, Ivánek R, Holková H, Jahnová H, van der Zee J, Staropoli JF, et al. Mutations in DNAJC5, encoding cysteine-string protein α, cause autosomal-dominant adult-onset neuronal ceroid lipofuscinosis. Am J Hum Genet 2011; 89:241-52; PMID:21820099; http://dx.doi.org/10.1016/j.ajhg.2011.07.003
48. Velinov M, Dolzhanskaya N, Gonzalez M, Powell E, Konidari I, Hulme W, Staropoli JF, Xin W, Wen GY, Barone R, et al. Mutations in the gene DNAJC5 cause autosomal dominant Kufs disease in a proportion of cases: study of the Parry family and 8 other families. PLoS One 2012; 7:e29729; PMID:22235333; http://dx.doi.org/10.1371/journal.pone.0029729
49. Greaves J, Salaun C, Fukata Y, Fukata M, Chamberlain LH. Palmitoylation and membrane interactions of the neuroprotective chaperone cysteine-string protein. J Biol Chem 2008; 283:25014-26; PMID:18596047; http://dx.doi.org/10.1074/jbc.M802140200
50. Greaves J, Lemonidis K, Gorleku OA, Cruchaga C, Grefen C, Chamberlain LH. Palmitoylation-induced aggregation of cysteine-string protein mutants that cause neuronal ceroid lipofuscinosis. J Biol Chem 2012; 287:37330-9; PMID:22902780; http://dx.doi.org/10.1074/jbc.M112.389098
51. Rozas JL, Gómez-Sánchez L, Mircheski J, Linares-Clemente P, Nieto-González JL, Vázquez ME, Luján R, Fernández-Chacón R. Motorneurons require cysteine string protein-α to maintain the readily releasable vesicular pool and synaptic vesicle recycling. Neuron 2012; 74:151-65; PMID:22500637; http://dx.doi.org/10.1016/j.neuron.2012.02.019
52. Zhang Y-Q, Henderson MX, Colangelo CM, Ginsberg SD, Bruce C, Wu T, Chandra SS. Identification of CSPα Clients Reveals a Role in Dynamin 1 Regulation. Neuron •••; 201:136-50
53. Huang K, Yanai A, Kang R, Arstikaitis P, Singaraja RR, Metzler M, Mullard A, Haigh B, Gauthier-Campbell C, Gutekunst CA, et al. Huntingtin-interacting protein HIP14 is a palmitoyl transferase involved in palmitoylation and trafficking of multiple neuronal proteins. Neuron 2004; 44:977-86; PMID:15603740; http://dx.doi.org/10.1016/j.neuron.2004.11.027
54. Kang R, Swayze R, Lise MF, Gerrow K, Mullard A, Honer WG, El-Husseini A. Presynaptic trafficking of synaptotagmin I is regulated by protein palmitoylation. J Biol Chem 2004; 279:50524-36; PMID:15355980; http://dx.doi.org/10.1074/jbc.M404981200
55. Wang JW, Sylwester AW, Reed D, Wu DAJ, Soll DR, Wu CF. Morphometric description of the wandering behavior in Drosophila larvae: aberrant locomotion in Na+ and K+ channel mutants revealed by computer-assisted motion analysis. J Neurogenet 1997; 11:231-54; PMID:10876655; http://dx.doi.org/10.3109/01677069709115098
56. Rivlin PK, Wyttenbach RA, Mitschelen MC, Hoy RR. Fruitfly: Discovering the neural basis of behavior through genetic dissection. Soc. Neurosci. Abstr. Program No. 29.11. Abstract Viewer/Itinerary Planner. Washington D.C.: Society for Neuroscience, 2004. Online.
57. Stewart BA, Atwood HL, Renger JJ, Wang J, Wu C-F. Improved stability of Drosophila larval neuromuscular preparations in haemolymph-like physiological solutions. J Comp Physiol A 1994; 175:179-91; PMID:8071894; http://dx.doi.org/10.1007/BF00215114